Benchmark calculations for polarization observables in three-nucleon scattering

A. Kievsky and M. Viviani
Istituto Nazionale di Fisica Nucleare, Piazza Torricelli 2, 56100 Pisa, Italy

S. Rosati
Dipartimento di Fisica, Universita' di Pisa, Piazza Torricelli 2, 56100 Pisa, Italy

D. Hüber
Los Alamos National Laboratory, M.S. B283, Los Alamos, New Mexico 87545

W. Glöckle and H. Kamada
Institut für Theoretische Physik II, Ruhr-Universität Bochum, D-44780 Bochum, Germany

H. Witała and J. Golak
Institute of Physics, Jagellonian University, PL-30059 Cracow, Poland

High precision benchmark calculations for phase shifts and mixing parameters as well as observables in elastic neutron-deuteron scattering below the deuteron breakup threshold are presented using a realistic nucleon-nucleon potential. Two totally different methods, one using a variational principle in configuration space and the other solving the Faddeev equations in momentum space, are used and compared to each other. The agreement achieved in phase shifts and mixing parameters as well as in the polarization observables is excellent. The extreme sensitivity of the vector analyzing power A_y to small changes of the phase shifts and mixing parameters is pointed out. [S0556-2813(98)07312-9]

I. INTRODUCTION

A complete theoretical description of the three-nucleon ($3N$) system is still limited by our knowledge of the nuclear interaction. Recently, progress has been achieved by optimally tuning various NN potential models to the NN data base, which lead to a fit with a χ^2 per datum very close to 1. Even by using these modern NN potentials in triton calculations [1] the well known underbinding problem is still present. The calculated binding energies lie between 7.6–8.0 MeV. A possible way to overcome this difficulty consists in including three-nucleon interaction (TNI) terms in the $3N$ Hamiltonian, usually fitted to reproduce the correct experimental binding energy of 8.48 MeV. There are various models for TNI, arising from the π-π exchange [2], exchanges of heavier mesons [3] or having more phenomenological forms [4]. The investigation of the TNI effects must not be limited to the $3N$ bound state but should be extended to the $3N$ continuum. A prerequisite to that is a well grounded theoretical approach and the numerical control of its application to $3N$ scattering problems. Under this respect, much progress has been made in recent years [5–8]. As shown in [8], the overall agreement to measured $3N$ observables using modern NN potentials is quite good, but there are exceptions. Among them we can recall the $3N$ nucleon vector analyzing power A_y, which depends very sensitively on the ^3P_j NN force components [9], or the deuteron vector analyzing power iT_{11}, which shows a similar sensitivity. Both these observables have specific dependencies in terms of $3N$ S-matrix elements: they are determined mainly by the ^4P_J-parameters

[10,11]. Such strong dependencies require very accurate calculations. The aim of the present article is to demonstrate that extremely accurate numerical results can be achieved. These two $3N$ observables A_y and iT_{11} are of special interest, since present theoretical descriptions are about 30% off the experimental data in the low energy region and up to now no explanation has been found for the discrepancy [9,12–14].

One way to parametrize the amplitude for elastic Nd scattering is in terms of the partial-wave decomposed S-matrix elements $S^J_{\lambda'\Sigma'\lambda\Sigma}$. Here J is the total $3N$ angular momentum, λ and λ' the orbital angular momenta of a nucleon in relation to the deuteron and Σ and Σ' the total spins of the deuteron and the third nucleon. The S-matrix elements can be expressed in terms of phase-shift and mixing parameters. As already stated above, the analyzing powers A_y and iT_{11} show extreme dependencies on some of them. As it will be discussed in the next section, differences of about 1% in some phase-shift parameters can lead to differences in these observables as large as 10% and more. Other observables, as the tensor analyzing powers and the spin-transfer and spin-correlation coefficients, are sensitive to states with high values of λ, typically $\lambda \geq 2$, which are also important when phase-shift analysis (PSA) are performed.

In the present work we provide benchmark calculations for $3N$ scattering observables as well as for S-matrix parameters below the deuteron breakup threshold using a realistic NN interaction. Two different techniques are used to calculate the S-matrix elements. The Bochum-Cracow group solves the Faddeev equations in momentum space as de-

scribed in [6] and [8]. The Pisa group uses the Kohn variational principle in configuration space [5,15,16]. Both techniques have been used in [17] but limiting the comparison just to phase-shift and mixing parameters for states with total angular momentum $J \leq 7/2$. Here we extend the investigation to a number of observables by taking into account also states with higher J values which are needed for a complete convergence of all considered observables. At the same time we increase the accuracy in order to demonstrate the numerical reliability of both methods to an unprecedented degree. Special emphasis is laid to the numerical accurate description of the vector analyzing power A_y, since it poses a severe theoretical puzzle.

The results obtained by the two techniques for the phase shift and mixing parameters are presented in the next section. Those for the observables are reported in Sec. III. The conclusions are the content of the final section.

II. PHASE SHIFT AND MIXING PARAMETERS

The two approaches used for numerical applications in this article have been described previously. The Pisa group uses the pair correlated hyperspherical harmonic (PHH) basis to expand the scattering wave function [5] and the corresponding S-matrix is obtained using the complex form of the Kohn variational principle [16]. The Bochum-Cracow group solves the Faddeev equations for the breakup operator in momentum space [6,8]. The complex transition matrix for elastic scattering is then gained by quadrature.

The comparison between the results of the two techniques has been performed using one of the Argonne NN potentials, namely the AV14 [18] one, which has all the complexities of a modern NN interaction built in. Our choice has been motivated by the fact that this potential was used in many benchmark calculations in the past, especially in [17]. The incident nucleon laboratory energy has been fixed at $E_{\text{lab}} = 3.0$ MeV, just below the deuteron breakup threshold.

In the correlated hyperspherical method the pattern of convergence for the S-matrix has been studied including in the n-d wave functions channels with increasing angular momenta values. Let us denote by l_α and L_α the orbital angular momentum quantum numbers associated to the Jacobi vectors of the $3N$ system in the channel α, and define $K_0 = l_\alpha + L_\alpha$. The choices $K_0 \leq 2(3)$, 4(5), 6(7) mean that all channels with $l_\alpha + L_\alpha \leq 2(3)$, 4(5), 6(7) have been included for positive (negative) parity states. Of course, the number of hyperspherical components for each channel has been increased until convergence has been reached. As an example, the numbers of the channels pertaining to the choices $K_0 = 2,4,6$, for the $J^\Pi = 1/2^+$ state, result to be $N_c = 10,18,26$, respectively. Channels with higher K_0 values were checked to give completely disregardable contributions.

In the Faddeev method in momentum space the convergence for the S-matrix is studied increasing the total two-body angular momentum j_{max} up to which the NN force is taken into account. We went up to $j_{\text{max}} = 8$ for $J = 1/2$ and 3/2. It turned out that with $j_{\text{max}} = 6$ a complete convergence for the phase-shifts and mixing parameters was achieved. So, $j_{\text{max}} = 6$ was used in the calculations for higher J values. As an example, the values $j_{\text{max}} = 2, 4, 6, 8$ for $J = 1/2$ correspond

to 18, 34, 50, 66 channels, respectively. For higher J's the number of channels increases up to 34, 98, 194, and 322, respectively.

The results for the phase-shift and mixing parameters are displayed in Table I for states up to $J = 9/2$. The Pisa numbers are calculated with $K_0 \leq 6(7)$ for the positive (negative) parity states and the Bochum-Cracow numbers with $j_{\text{max}} \leq 6$. For states with higher J values the nuclear exchange term PG_0^{-1} as given in Eq. (2.14) of Ref. [17] is sufficient, as has been standard use in the Bochum-Cracow approach. In the notation of the Pisa group this amounts to the following easy manner to compute the S-matrix. In the states with high relative angular momentum λ the incident nucleon and the deuteron are well separated due to centrifugal barrier effects. Therefore, the asymptotic form of the wave function gives essentially a correct description of the system. The reactance matrix (K-matrix) of the system is given in this approximation (symmetrized Born approximation) by

$$K_{\lambda'\Sigma'\lambda\Sigma}^J = \sum_{ij} \langle \lambda'\Sigma',i;J|H-E|\lambda\Sigma,j;J\rangle, \quad (1)$$

where the $|\lambda\Sigma,i;J\rangle$ describes a free incident nucleon i and a deuteron in a relative angular momentum λ state. Σ is the total spin of the deuteron and the nucleon. Using the fact that the asymptotic state is solution of the free Hamiltonian plus the interaction between particles j,k, the following simpler form is obtained:

$$K_{\lambda'\Sigma'\lambda\Sigma}^J = 3\sum_i \sum_{j\neq 1} \langle \lambda'\Sigma',i;J|V(2,3)|\lambda\Sigma,j;J\rangle. \quad (2)$$

A further approximation consists in retaining the most important term (Born approximation):

$$K_{\lambda'\Sigma'\lambda\Sigma}^J = 3\sum_{j\neq 1} \langle \lambda'\Sigma',1;J|V(2,3)|\lambda\Sigma,j;J\rangle. \quad (3)$$

This form is equivalent to the nuclear exchange term used by the Bochum-Cracow group:

$$K_{\lambda'\Sigma'\lambda\Sigma}^J = 3\langle \lambda'\Sigma',1;J|PG_0^{-1}|\lambda\Sigma,1;J\rangle. \quad (4)$$

The S-matrix is simply obtained using the relation $S = (1 + iK)(1 - iK)^{-1}$. For the low energy used in this study, the Born approximation has been adopted for states with angular momenta $J \geq 11/2$. The results obtained in this approximation for the phase-shift and mixing parameters by the two groups completely overlap and are given in Table II for states from $J = 11/2$ up to $J = 15/2$. As it will be shown in the next section, higher J states give disregardable contributions to the observables at the energy considered here.

The numbers presented in Table I, obtained by the two different methods, agree between each other to within less than 0.1%. There are a few exceptions, where the differences go up to 0.7%. This clearly demonstrates the power and reliability of both methods, which are totally different also under the respect of the adopted numerical procedures. The comparison of our new results to the older ones in Table II of Ref. [17] gives a clear idea of the improvements in the numerical accuracy. The phases given in Table II of [17] by the

TABLE I. Phase shifts and mixing parameters in terms of the quantum numbers j_{max} and K_0. The numbers in parenthesis for K_0 refer to odd parity states.

J^Π	$\delta_{\Sigma\lambda}$	Bochum			Pisa		
		$j_{max}=2$	$j_{max}=4$	$j_{max}=6$	$K_0=2(3)$	$K_0=4(5)$	$K_0=6(7)$
$\frac{1}{2}^+$	$\delta_{(3/2)2}$	-3.897	-3.903	-3.904	-3.899	-3.905	-3.905
	$\delta_{(1/2)0}$	-35.35	-34.84	-34.81	-35.33	-34.81	-34.81
	η	1.179	1.247	1.251	1.271	1.252	1.253
$\frac{1}{2}^-$	$\delta_{(1/2)1}$	-7.479	-7.524	-7.529	-7.534	-7.533	-7.533
	$\delta_{(3/2)1}$	25.10	25.06	25.06	25.04	25.05	25.05
	ϵ	7.268	7.253	7.254	7.252	7.255	7.255
$\frac{3}{2}^+$	$\delta_{(3/2)0}$	-70.47	-70.48	-70.48	-70.52	-70.50	-70.50
	$\delta_{(1/2)2}$	2.439	2.422	2.421	2.421	2.420	2.420
	$\delta_{(3/2)2}$	-4.204	-4.214	-4.215	-4.216	-4.216	-4.216
	η	-0.3963	-0.3889	-0.3881	-0.3869	-0.3873	-0.3874
	ϵ	0.7745	0.7766	0.7785	0.7747	0.7801	0.7800
	ξ	1.451	1.438	1.438	1.429	1.438	1.438
$\frac{3}{2}^-$	$\delta_{(3/2)3}$	0.9466	0.9443	0.9441	0.9425	0.9436	0.9436
	$\delta_{(1/2)1}$	-7.145	-7.186	-7.191	-7.201	-7.195	-7.195
	$\delta_{(3/2)1}$	26.44	26.42	26.41	26.39	26.40	26.41
	η	-3.854	-3.813	-3.809	-3.819	-3.806	-3.805
	ϵ	-2.751	-2.764	-2.765	-2.762	-2.768	-2.765
	ξ	-0.2400	-0.2567	-0.2574	-0.2577	-0.2573	-0.2575
$\frac{5}{2}^+$	$\delta_{(3/2)4}$	-0.2105	-0.2109	-0.2110	-0.2113	-0.2112	-0.2111
	$\delta_{(1/2)2}$	2.401	2.388	2.386	2.382	2.385	2.385
	$\delta_{(3/2)2}$	-4.558	-4.567	-4.567	-4.571	-4.569	-4.569
	η	-2.084	-2.146	-2.152	-2.167	-2.157	-2.157
	ϵ	-0.3450	-0.3266	-0.3264	-0.3387	-0.3275	-0.3280
	ξ	-0.7637	-0.7379	-0.7356	-0.7343	-0.7365	-0.7363
$\frac{5}{2}^-$	$\delta_{(3/2)1}$	26.40	26.39	26.38	26.32	26.35	26.37
	$\delta_{(1/2)3}$	-0.4723	-0.4760	-0.4765	-0.4771	-0.4768	-0.4767
	$\delta_{(3/2)3}$	0.9757	0.9720	0.9716	0.9694	0.9711	0.9712
	η	-0.3475	-0.3596	-0.3605	-0.3593	-0.3609	-0.3609
	ϵ	0.5007	0.5165	0.5168	0.5188	0.5165	0.5165
	ξ	0.9566	0.9832	0.9844	0.9943	0.9847	0.9845
$\frac{7}{2}^+$	$\delta_{(3/2)2}$	-4.140	-4.142	-4.143	-4.151	-4.145	-4.144
	$\delta_{(1/2)4}$	0.1107	0.1104	0.1103	0.1100	0.1103	0.1102
	$\delta_{(3/2)4}$	-0.2200	-0.2204	-0.2205	-0.2208	-0.2207	-0.2209
	η	-0.5130	-0.4923	-0.4905	-0.4868	-0.4894	-0.4895
	ϵ	0.3575	0.3694	0.3683	0.3695	0.3680	0.3686
	ξ	1.266	1.225	1.221	1.219	1.222	1.222
$\frac{7}{2}^-$	$\delta_{(3/2)5}$	0.04950	0.04947	0.04946	0.04944	0.04944	0.04944
	$\delta_{(1/2)3}$	-0.4654	-0.4683	-0.4688	-0.4695	-0.4690	-0.4689
	$\delta_{(3/2)3}$	1.030	1.027	1.026	1.024	1.026	1.026
	η	-2.334	-2.311	-2.304	-2.298	-2.301	-2.308
	ϵ	-0.2120	-0.2505	-0.2527	-0.2500	-0.2524	-0.2510
	ξ	-0.7720	-0.7790	-0.7823	-0.7842	-0.7826	-0.7873

TABLE I. *(Continued).*

J^Π	$\delta_{\Sigma\lambda}$	Bochum			Pisa		
		$j_{max}=2$	$j_{max}=4$	$j_{max}=6$	$K_0=2(3)$	$K_0=4(5)$	$K_0=6(7)$
$\frac{9}{2}^+$	$\delta_{(3/2)6}$	-0.01170	-0.01170	-0.01170	-0.01170	-0.01170	-0.01170
	$\delta_{(1/2)4}$	0.1088	0.1086	0.1085	0.1082	0.1084	0.1084
	$\delta_{(3/2)4}$	-0.2292	-0.2293	-0.2294	-0.2297	-0.2297	-0.2297
	η	-2.214	-2.218	-2.223	-2.231	-2.227	-2.226
	ϵ	-0.2049	-0.1983	-0.1954	-0.1947	-0.1897	-0.1954
	ξ	-0.8291	-0.8289	-0.8262	-0.8251	-0.8252	-0.8259
$\frac{9}{2}^-$	$\delta_{(3/2)3}$	0.9441	0.9440	0.9439	0.9413	0.9435	0.9435
	$\delta_{(1/2)5}$	-0.02550	-0.02550	-0.02552	-0.02553	-0.02553	-0.02553
	$\delta_{(3/2)5}$	0.05151	0.05150	0.05149	0.05147	0.05147	0.05147
	η	-0.4781	-0.4841	-0.4863	-0.4887	-0.4867	-0.4866
	ϵ	0.3316	0.3268	0.3277	0.3273	0.3275	0.3276
	ξ	1.146	1.156	1.161	1.164	1.162	1.162

two methods show some disagreements in the third digit and, sometimes, even in the second digit. Now we have much better agreement. Only very seldom is there disagreement in the third digit of a mixing parameter. So, we have now an improved agreement in the phase-shift parameters of one more digit with respect to [17].

A direct comparison of the *S*-matrix represents a severe numerical test for both methods. The *S*-matrix is part of the wave function and its elements are very sensitive to the different contributions of the potential. This is put in evidence in Table I where some parameters converged only after the inclusion of high components in the expansion. To construct the subtle details of the wave function is always a difficult task. To this end, extended and denser grids of points have been used in the numerical solution of the equations. Stable numerical results have been obtained using the integral equations for calculating the *S*-matrix (Bochum group) and the Kohn second order estimate (Pisa group). Fortunately, as shown in the next section, for the observables there is not such a strong dependence on the details of the wave function and a number of grid points like those ones used in previous works is adequate.

TABLE II. Phase shifts and mixing parameters from $J=11/2$ to $J=15/2$ in Born approximation.

J^Π	$\delta_{\Sigma\lambda}$	Bochum-Cracow-Pisa	J^Π	$\delta_{\Sigma\lambda}$	Bochum-Cracow-Pisa
$\frac{11}{2}^+$	$\delta_{(3/2)4}$	-0.2135	$\frac{11}{2}^-$	$\delta_{(3/2)7}$	0.00280
	$\delta_{(1/2)6}$	0.00603		$\delta_{(1/2)5}$	-0.02513
	$\delta_{(3/2)6}$	-0.01216		$\delta_{(3/2)5}$	0.05311
	η	-0.4942		η	-2.204
	ϵ	0.2978		ϵ	-0.1785
	ξ	1.142		ξ	-0.8481
$\frac{13}{2}^+$	$\delta_{(3/2)8}$	-0.00067	$\frac{13}{2}^-$	$\delta_{(3/2)5}$	0.04968
	$\delta_{(1/2)6}$	0.00593		$\delta_{(1/2)7}$	-0.00144
	$\delta_{(3/2)6}$	-0.01249		$\delta_{(3/2)7}$	0.00290
	η	-2.185		η	-0.4975
	ϵ	-0.1660		ϵ	0.2779
	ξ	-0.8640		ξ	1.125
$\frac{15}{2}^+$	$\delta_{(3/2)6}$	-0.01173	$\frac{15}{2}^-$	$\delta_{(3/2)9}$	0.00016
	$\delta_{(1/2)8}$	0.00035		$\delta_{(1/2)7}$	-0.00141
	$\delta_{(3/2)8}$	-0.00070		$\delta_{(3/2)7}$	0.00297
	η	-0.4998		η	-2.170
	ϵ	0.2634		ϵ	-0.1570
	ξ	1.111		ξ	-0.8752
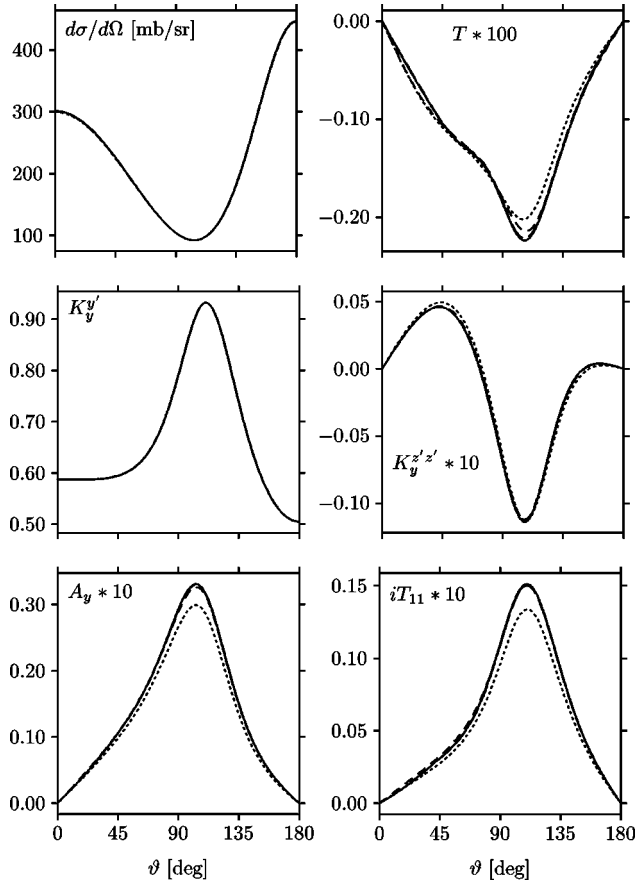
FIG. 1. The differential cross section $d\sigma/d\Omega$, the tensor spin-correlation coefficient T, the nucleon-to-nucleon vector spin-transfer coefficient $K_y^{y'}$, the nucleon-to-deuteron tensor spin-transfer coefficient $K_y^{z'z'}$, and the nucleon and deuteron vector analyzing powers A_y and iT_{11} at $E_{lab}=3$ MeV. The solid lines are obtained from the Bochum-Cracow phases of this work, with the potential switched on up to $J=9/2$ and the nucleon exchange term taken into account from $J=11/2$ till $15/2$. The long-dashed lines are the same but obtained from the Pisa phases. The solid and long-dashed lines are always indistinguishable from each other. The short-dashed line is obtained for $J^{\Pi}=1/2^{\pm}$, $3/2^{\pm}$, $5/2^{\pm}$, and $7/2^{+}$ from the Bochum-Cracow phases of Ref. [17] and otherwise the phases from this paper. The dotted lines are the same but obtained from the corresponding Pisa phases.

FIG. 2. The differential cross section $d\sigma/d\Omega$, the nucleon vector analyzing power A_y, the deuteron tensor analyzing power T_{21}, the nucleon-to-deuteron tensor spin-transfer coefficient $K_y^{z'z'}$ and the two tensor spin-correlation coefficients S and T, calculated by increasing the maximum allowed two-body angular momentum j_{max}. Solid, long-dashed, and short-dashed lines refer to $j_{max}=6$, 4, and 2, respectively. Note that the solid and long-dashed lines do always completely overlap.

III. 3N ELASTIC SCATTERING OBSERVABLES

We begin by showing in Fig. 1 the perfect agreement among the observables evaluated by the two methods. The two results for the observables are represented by the solid and long-dashed lines in Fig. 1, which are always indistinguishable from each other. These calculations are based on the phases of Table I evaluated with highest accuracy.

However we can relax those high requests and still keep a very good agreement among the predictions of the two methods. For the Bochum-Cracow calculations we can lower the two-nucleon angular momentum j_{max} up to which we keep the NN force different from zero from $j_{max}=6$ to $j_{max}=3$ and still describe the observables within about 1 percent. Some examples are shown in Fig. 2 calculated with $j_{max}=2$, 4, and 6, respectively. The lines for $j_{max}=4$ and 6 are

indistinguishable, whereas the lines for $j_{max}=2$ exhibits small deviations from the other lines for some of the observables. The changes in the phases gained by going to j_{max} higher than 3 cancel out in the observables or occur for small phase-shifts and mixing parameters which are not so important for the determination of the observables. The same phenomenon can be seen by increasing the numerical accuracy. Though a lot of phase-shifts and mixing parameters show sensitivity to numerical details, the observables do not. For the Pisa approach most of the large phase-shifts are already converged for $K_0=4(5)$ (see Table I), whereas the smallest observables converge only for $K_0=6(7)$, as shown in Fig. 3.

Next let us regard the convergence of the observables with respect to J and λ separately. Since it does not matter which of the two sets of phases we are using, we carry through that study with the Bochum-Cracow phases.

Let us start with the convergence in J. It turns out that the convergence in J can be described in a very systematic way. For spin observables whose magnitude is about 0.1, or greater than that, the convergence is reached already for $J \leqslant 11/2$. In Fig. 4 we show as a typical example $K_y^{y'}$. For the next class of observables with magnitudes about 10 times
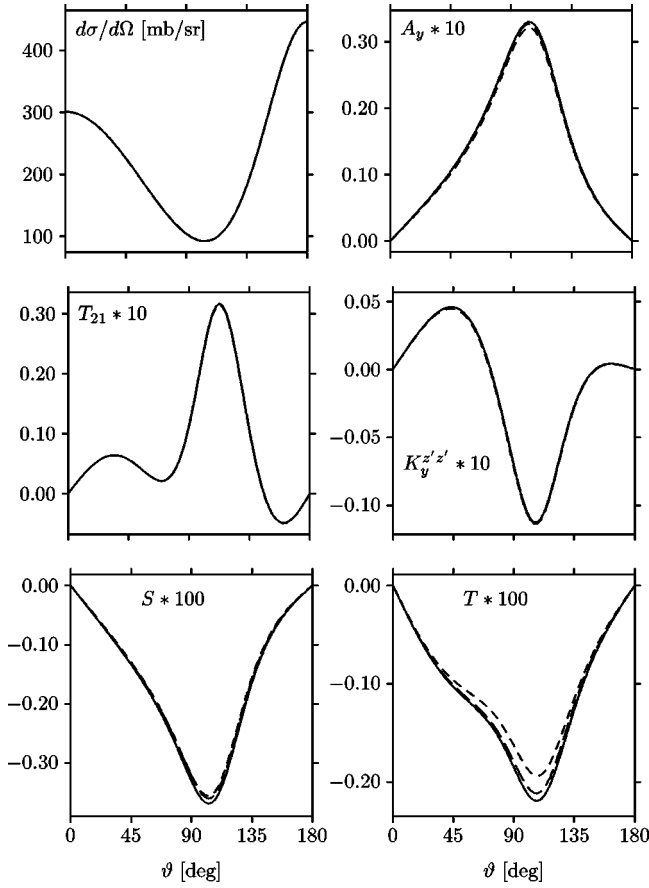
FIG. 3. The differential cross section $d\sigma/d\Omega$, the nucleon vector analyzing power A_y, the deuteron tensor analyzing power T_{21}, the nucleon-to-deuteron tensor spin-transfer coefficient $K_y^{z'z'}$ and the two tensor spin-correlation coefficients S and T, calculated by increasing the maximum allowed K_0 in the expansion of the wave function. Solid, long-dashed, and short-dashed lines correspond to maximum $K_0 = 6(7), 4(5), 2(3)$.

smaller convergence is found for $J \leq 13/2$. Here we have chosen as a typical example A_y also shown in Fig. 4. For the next class, again by about a factor of 10 smaller, even $J \leq 15/2$ is not quite sufficient, as can be seen in the example T in Fig. 4, and states up to $J = 25/2$ have to be taken into account. Thus the convergence in J is strongly correlated to the magnitudes of the observables.

Let us now examine the convergence with respect to λ. For a given J and parity Π, the S-matrix elements are all coupled to each other. Therefore, limiting the calculation of the observables by a maximal λ (instead of a maximal J) means that for some J^Π states, only parts of the corresponding S-matrices are taken into account. However, this procedure does not harm and one gets always a very nice convergence. Actually, at these low energies, the contributions of the waves with large values of λ are suppressed by the centrifugal barrier, and therefore the convergence in λ is usually faster than that in J.

As an example we show in Fig. 5 the $K_y^{z'z'}$ and T observables. As can be seen in the figure, for $\lambda \leq 5$ T is already converged, and $\lambda \leq 4$ is not too bad, either. As one can see for example from Table I, $\lambda \leq 5$ means that the highest J
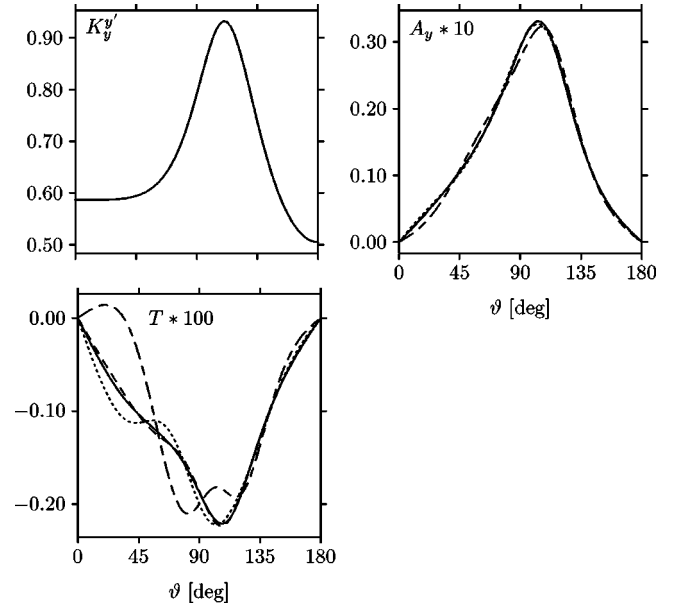
FIG. 4. Convergence in J for the nucleon-to-nucleon vector spin-transfer coefficient $K_y^{y'}$, the nucleon vector analyzing power A_y, and the tensor spin-correlation coefficient T. Shown is the result obtained from the phases with $J \leq 25/2$ (solid line), $J \leq 15/2$ (short-dashed line), $J \leq 13/2$ (dotted line), and $J \leq 11/2$ (long-short-dashed line).

taken into account is 13/2. On the other hand the much larger observable $K_y^{z'z'}$ is fully converged only for $\lambda \leq 6$, which means one needs phases up to $J = 15/2$. In J this observable reaches convergence earlier, for $J \leq 13/2$. But this is the exception. In most cases the convergence in λ is faster than in J.

Now let us demonstrate the extreme sensitivity of A_y with respect to tiny changes of some phase shift parameters, namely the ^4P_J phase-shifts and the $\epsilon^{3/2-}$ mixing parameter. We modified them individually by 1%. The effect on A_y is shown in Table III (see also Table 2 in Ref. [10]). Clearly the sensitivity of A_y to the ^4P_J phase-shifts is quite dramatic—an enlargement factor of up to nearly 20 from changes in the phases to changes in the observable are found.
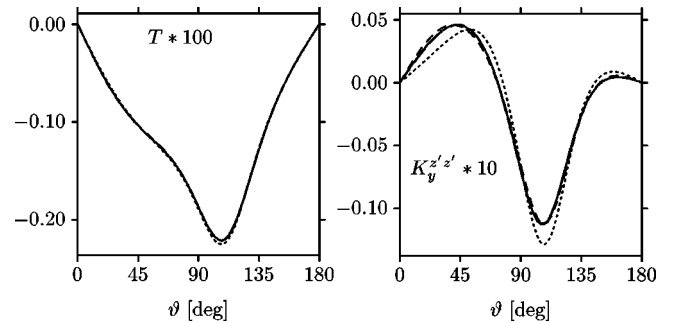
FIG. 5. Convergence in λ for the tensor spin-correlation coefficient T and the nucleon-to-deuteron tensor spin-transfer coefficient $K_y^{z'z'}$. Shown are the results obtained from the phases with $\lambda \leq 6$ (long-dashed line), $\lambda \leq 5$ (short-dashed line), and $\lambda \leq 4$ (dotted line). The solid line is the same as in Fig. 4,

TABLE III. The effect of 1% changes in the phases to which A_y is most sensitive. Given is the value of A_y in its maximum as well as the change in percent in the maximum.

	$A_y|_{max}$	%
AV14	0.3306	
$^4P_{1/2} \times 1.01$	0.2960	-11.7
$^4P_{3/2} \times 1.01$	0.3083	-7.2
$^4P_{5/2} \times 1.01$	0.4051	18.4
$\epsilon^{3/2-} \times 1.01$	0.3362	1.7

There are no such extremely strong sensitivities to the NN ^3P_j phase-shifts [10], although they alone determine A_y. In [10] the biggest enlargement factor was reported for $^3P_0$ to be 3.5. In view of that extreme sensitivity it is interesting to see which A_y would result by using the phases of Ref. [17], which were calculated not with such an extreme accuracy as in this article. Thereby it is interesting to note how the more accurate calculations in this study change all of these four parameters which dominate A_y for both approaches compared to the older and less accurate numbers in [17]: the changes are 0.24% (0.20%) for $^4P_{1/2}$, 0.42% (0.42%) for $^4P_{3/2}$, 0.30% (0.65%) for $^4P_{5/2}$ and 0.55% (1.65%) for $\epsilon^{3/2-}$ in the Bochum-Cracow (Pisa) case. Now the A_y resulting from the phases of [17] is shown in Fig. 1 (beside other observables) in comparison to the present best result. We see a small shift for the Bochum-Cracow result and a larger one for the Pisa result. This can be illustrated further by assuming that A_y changes linearly with changes of the phases around their present values. Using Table III together with the small changes of the present phases to the ones of Ref. [17] one indeed finds that A_y should change by about 10% (1%) for the Pisa (Bochum) case. In other words in one case we see a stability for the resulting observable, in the other case not. The simple reason is that the expansion in the PHH components in [17] was truncated in a nonuniform manner for the different states and in [17] it was not foreseen that even those small changes in the phases would effect certain observables in a magnified manner. On the other hand if a consistent treatment of all states is performed the individual changes of the phases are smoothed out in the observables, as it was the case for the Bochum-Cracow calculation in Ref. [17]. In the Pisa group papers successive to Ref. [17] and in the present paper the PHH expansion has been consistently carried through for all states with a correct calculation of A_y.

IV. SUMMARY AND CONCLUSIONS

In the present paper benchmark calculations for phase-shift and mixing parameters, as well as for observables in elastic neutron-deuteron scattering below the deuteron breakup threshold are presented. We used the realistic AV14 NN potential. Two *ab initio* completely different methods have been used to calculate the quantities of interest. The approach of the Pisa group is based on the correlated hyperspherical expansion of the wave function in configuration space and uses the complex Kohn variational principle to determine the S- or the K-matrix. The approach of the Bochum-Cracow group is based on an exact technique for solving the Faddeev equations in momentum space.

The results obtained for the phase-shift and mixing parameters by means of the two approaches show nearly perfect agreement. Also the calculated observables agree very well with each other. This demonstrates that both the variational approach of the Pisa group and the integral equation method of the Bochum-Cracow group are equally well suited for high accuracy calculations of the elastic nd scattering observables below the breakup threshold.

The comparison with the older results of Ref. [17] shows that the numerical accuracy in the phase-shift and mixing parameters has increased by one more digit. The changes in the phase-shifts had only very small effects on the results for the observables of the Bochum-Cracow group. The situation was different for the Pisa results, since in Ref. [17] the phases were evaluated with different accuracy requirements for the different states and an observable like A_y which exhibits extreme sensitivity does not tolerate that. This shows that it is important to construct the observables by using S-matrix elements calculated at the same approximation level. In this case, in fact, a more rapid convergence with respect to the number of terms included in the internal structure of the n-d states and a lower sensitivity to the numerical accuracy is achieved for the observables. In fact, the S-matrix elements are part of the wave function and therefore rather sensitive to the subtle aspect of the structure of the state. On the contrary, the observables are average quantities where the small details of the wave function are somewhat smeared out.

Also the convergence of the observables along the total three-body angular momentum J and the relative angular momentum λ has been studied. We found that the convergence of the observables with the total three-body angular momentum J is strongly correlated to the magnitude of the observables. Though the convergence of the observables with the angular momentum λ is in most cases faster than in J, it is less systematic and has therefore to be checked with more care. Therefore a PSA has to treat the more phase-shifts as free parameters the smaller the considered observables are.

In the present paper, attention has been paid only to a realistic two nucleon interaction without the inclusion of TNI terms. This will be the object of a future investigation.

In conclusion, n-d scattering states at energies below the deuteron breakup threshold can be constructed equally accurately by the two methods presented. It is grateful that the phase-shift and mixing parameters can be calculated within a precision of about 0.1%, comparable to the one obtainable for bound states.

[1] A. Nogga, D. Hüber, H. Kamada, and W. Glöckle, Phys. Lett. B **409**, 19 (1997).

[2] S. A. Coon *et al.*, Nucl. Phys. **A317**, 242 (1979); S. A. Coon and W. Glöckle, Phys. Rev. C **23**, 1790 (1981).

[3] S. A. Coon and M. T. Peña, Phys. Rev. C **48**, 2559 (1993).

[4] B. S. Pudliner, V. R. Pandharipande, J. Carlson, S. C. Pieper, and R. B. Wiringa, Phys. Rev. C **56**, 1720 (1997).

[5] A. Kievsky, M. Viviani, and S. Rosati, Nucl. Phys. **A577**, 511 (1994); A. Kievsky, M. Viviani, and S. Rosati, Phys. Rev. C **52**, R15 (1995).

[6] H. Wital̷a, W. Glöckle, and Th. Cornelius, Few-Body Syst., Suppl. **2**, 555 (1987); H. Wital̷a, Th. Cornelius, and W. Glöckle, Few-Body Syst. **3**, 123 (1988).

[7] D. Hüber, H. Wital̷a, and W. Glöckle, Few-Body Syst. **14**, 171 (1993); D. Hüber, H. Kamada, H. Wital̷a, and W. Glöckle, Acta Phys. Pol. B **28**, 1677 (1997); D. Hüber, H. Wital̷a, A. Nogga, W. Glöckle, and H. Kamada, Few-Body Syst. **22**, 107 (1997).

[8] W. Glöckle, H. Wital̷a, D. Hüber, H. Kamada, and J. Golak, Phys. Rep. **274**, 107 (1996).

[9] H. Wital̷a and W. Glöckle, Nucl. Phys. **A577**, 48 (1991).

[10] D. Hüber, J. Golak, H. Wital̷a, W. Glöckle, and H. Kamada, Few-Body Syst. **19**, 175 (1995).

[11] A. Kievsky, S. Rosati, W. Tornow, and M. Viviani, Nucl. Phys. **A607**, 402 (1996).

[12] H. Wital̷a, D. Hüber, and W. Glöckle, Phys. Rev. C **49**, R14 (1994).

[13] W. Tornow, H. Wital̷a, and A. Kievsky, Phys. Rev. C **57**, 555 (1998).

[14] D. Hüber and J. L. Friar, Phys. Rev. C **58**, 674 (1998).

[15] A. Kievsky, M. Viviani, and S. Rosati, Nucl. Phys. **A551**, 241 (1993).

[16] A. Kievsky, Nucl. Phys. **A624**, 125 (1997).

[17] D. Hüber, W. Glöckle, J. Golak, H. Wital̷a, H. Kamada, A. Kievsky, M. Viviani, and S. Rosati, Phys. Rev. C **51**, 1100 (1995).

[18] R. B. Wiringa, R. A. Smith, and T. L. Ainsworth, Phys. Rev. C **29**, 1207 (1984).